2. Light and Matter

In this and the following chapter, we will discuss basic phenomena occurring when matter is exposed to light. While here we will be concerned with various actions of matter on light, the opposite effect will be discussed in Chap. 3. Matter can act on electromagnetic radiation in manifold ways. In Fig. 2.1, a typical situation is shown, where a light beam is incident on a slice of matter. In principle, three effects exist which may interfere with its undisturbed propagation:

– reflection and refraction,
– absorption,
– scattering.

Reflection and refraction are strongly related to each other by *Fresnel's laws*. Therefore, these two effects will be addressed in the same section. In Fig. 2.1, refraction is accounted for by a displacement of the transmitted beam. In medical laser applications, however, refraction plays a significant role only when irradiating transparent media like corneal tissue. In opaque media, usually, the effect of refraction is difficult to measure due to absorption and scattering.

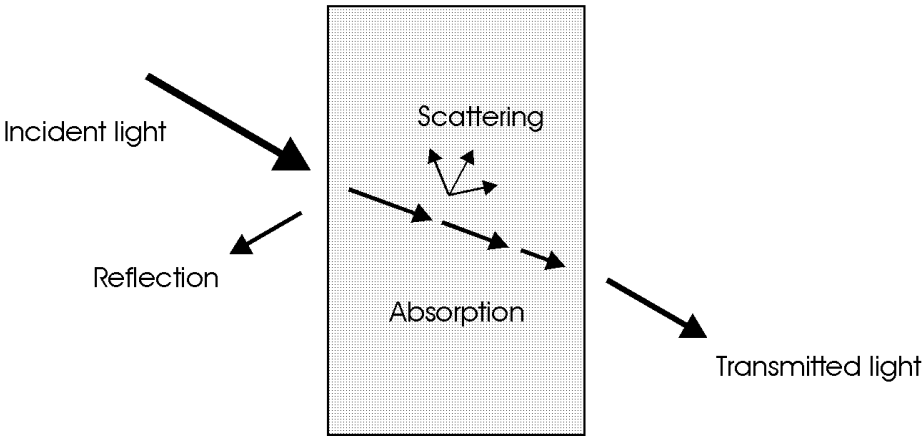

Fig. 2.1. Geometry of reflection, refraction, absorption, and scattering

Only nonreflected and nonabsorbed or forward scattered photons are transmitted by the slice and contribute to the intensity detected behind the slice. The ratio of transmitted and incident intensities is called *transmittance*. Which of the losses – reflection, absorption, or scattering – is dominant primarily depends on the type of material and the incident wavelength. As we will encounter in the following sections, the wavelength is a very important parameter indeed. It determines the index of refraction as well as the absorption and scattering coefficients. The index of refraction governs the overall reflectivity of the target. This index strongly depends on wavelength in regions of high absorption only. The scattering coefficient, on the other hand, can scale inversely with the fourth power of wavelength as will be evaluated in Sect. 2.3 when discussing Rayleigh scattering.

In laser surgery, knowledge of absorbing and scattering properties of a selected tissue is essential for the purpose of predicting successful treatment. The index of refraction might be of considerable interest when applying laser radiation to highly reflecting surfaces such as metallic implants in dentistry or orthopedics. In general, however, no specific kind of target or biological tissue will be assumed unless otherwise stated in certain figures or tables. Instead, emphasis is put on general physical relations which apply for most solids and liquids. In reality, of course, limitations are given by the inhomogeneity of biological tissue which are also responsible for our inability to provide other than mean tissue parameters.

2.1 Reflection and Refraction

Reflection is defined as the returning of electromagnetic radiation by surfaces upon which it is incident. In general, a reflecting surface is the physical boundary between two materials of different indices of refraction such as air and tissue. The simple law of reflection requires the wave normals of the incident and reflected beams and the normal of the reflecting surface to lie within one plane, called the *plane of incidence*. It also states that the reflection angle θ' equals the angle of incidence θ as shown in Fig. 2.2 and expressed by

$$\theta = \theta' \,. \tag{2.1}$$

The angles θ and θ' are measured between the surface normal and the incident and reflected beams, respectively. The surface itself is assumed to be smooth, with surface irregularities being small compared to the wavelength of radiation. This results in so-called *specular reflection*.

In contrast, i.e. when the roughness of the reflecting surface is comparable or even larger than the wavelength of radiation, *diffuse reflection* occurs. Then, several beams are reflected which do not necessarily lie within the plane of incidence, and (2.1) no longer applies. Diffuse reflection is a common phenomenon of all tissues, since none of them is provided with highly polished

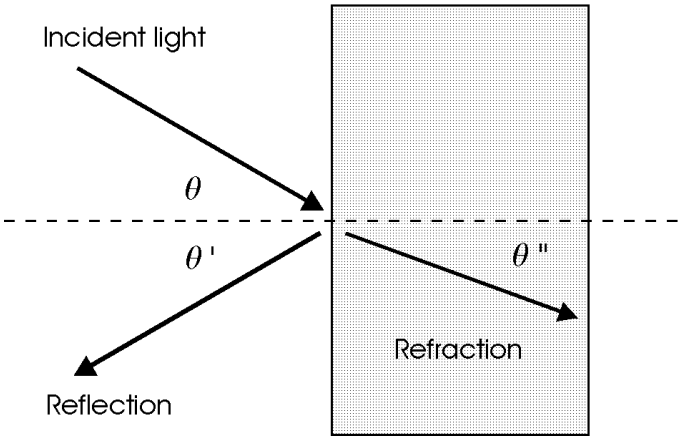

Fig. 2.2. Geometry of specular reflection and refraction

surfaces such as optical mirrors. Only in special cases such as wet tissue surfaces might specular reflection surpass diffuse reflection.

Refraction usually occurs when the reflecting surface separates two media of different indices of refraction. It originates from a change in speed of the light wave. The simple mathematical relation governing refraction is known as *Snell's law*. It is given by

$$\frac{\sin\theta}{\sin\theta''} = \frac{v}{v'} \ , \tag{2.2}$$

where θ'' is the angle of refraction, and v and v' are the speeds of light in the media before and after the reflecting surface, respectively. Since the corresponding indices of refraction are defined by

$$n = \frac{c}{v} \ , \tag{2.3}$$

$$n' = \frac{c}{v'} \ ,$$

where c denotes the speed of light in vacuum, (2.2) turns into

$$n \sin\theta = n' \sin\theta'' \ . \tag{2.4}$$

Only for $\sin\theta > n'/n$ can (2.4) not be fulfilled, meaning that refraction will not occur. This event is also referred to as *total reflection*.

The *reflectivity* of a surface is a measure of the amount of reflected radiation. It is defined as the ratio of reflected and incident electric field amplitudes. The *reflectance* is the ratio of the correponding intensities and is thus equal to the square of the reflectivity. Reflectivity and reflectance depend on the angle of incidence, the polarization of radiation, and the indices of

refraction of the materials forming the boundary surface. Relations for reflectivity and refraction are commonly known as *Fresnel's laws*. In this book, we will merely state them and consider their principal physical impact. Exact derivations are found elsewhere, e.g. in books dealing with electrodynamics. Fresnel's laws are given by

$$\frac{E_\mathrm{s}{}'}{E_\mathrm{s}} = -\frac{\sin(\theta-\theta'')}{\sin(\theta+\theta'')}\,, \tag{2.5}$$

$$\frac{E_\mathrm{p}{}'}{E_\mathrm{p}} = \frac{\tan(\theta-\theta'')}{\tan(\theta+\theta'')}\,, \tag{2.6}$$

$$\frac{E_\mathrm{s}{}''}{E_\mathrm{s}} = \frac{2\,\sin\theta''\,\cos\theta}{\sin(\theta+\theta'')}\,, \tag{2.7}$$

$$\frac{E_\mathrm{p}{}''}{E_\mathrm{p}} = \frac{2\,\sin\theta''\,\cos\theta}{\sin(\theta+\theta'')\;\cos(\theta-\theta'')}\,, \tag{2.8}$$

where E, E', and E'' are amplitudes of the electric field vectors of the incident, reflected, and refracted light, respectively. The subscripts "s" and "p" denote the two planes of oscillation with "s" being perpendicular to the plane of incidence – from the German *senkrecht* – and "p" being parallel to the plane of incidence.

Further interaction of incident light with the slice of matter is limited to the refracted beam. One might expect that the intensity of the refracted beam would be complementary to the reflected one so that the addition of both would give the incident intensity. However, this is not correct, because intensity is defined as the power per unit area, and the cross-section of the refracted beam is different from that of the incident and reflected beams except at normal incidence. It is only the total energy in these beams that is conserved. The reflectances in either plane are given by

$$R_\mathrm{s} = \left(\frac{E_\mathrm{s}{}'}{E_\mathrm{s}}\right)^2\,, \tag{2.9}$$

$$R_\mathrm{p} = \left(\frac{E_\mathrm{p}{}'}{E_\mathrm{p}}\right)^2\,. \tag{2.10}$$

In Fig. 2.3, the reflectances R_s and R_p are plotted as a function of the angle of incidence. It is assumed that $n = 1$ and $n' = 1.33$ which are the indices of refraction of air and water, respectively. Thus, Fig. 2.3 especially describes the specular reflectance on wet surfaces.

The angle at which $R_\mathrm{p} = 0$ is called the *Brewster angle*. In the case of water, it is equal to 53°. At normal incidence, i.e. $\theta = 0$, the reflectances in either plane are approximately 2 %. This value is not directly evident from (2.5) and (2.6), since insertion of $\theta = \theta'' = 0$ gives an indeterminate result. It can be evaluated, however, as follows. Since both θ and θ'' become

very small when approaching normal incidence, we may set the tangents in (2.6) equal to the sines and obtain

$$R_\mathrm{p} \simeq R_\mathrm{s} = \frac{\sin^2(\theta - \theta'')}{\sin^2(\theta + \theta'')} = \left(\frac{\sin\theta\ \cos\theta'' - \cos\theta\ \sin\theta''}{\sin\theta\ \cos\theta'' + \cos\theta\ \sin\theta''}\right)^2 . \qquad (2.11)$$

When dividing numerator and denominator of (2.11) by $\sin\theta''$ and replacing $\sin\theta/\sin\theta''$ by n', i.e. assuming $n = 1$, it reduces to

$$R_\mathrm{p} \simeq R_\mathrm{s} = \left(\frac{n'\cos\theta'' - \cos\theta}{n'\cos\theta'' + \cos\theta}\right)^2 \simeq \left(\frac{n'-1}{n'+1}\right)^2 . \qquad (2.12)$$

The approximate equality becomes exact within the limit of normal incidence. Thus, inserting $n' = 1.33$ yields

$$R_\mathrm{p} \simeq R_\mathrm{s} \simeq 2\,\% .$$

In several cases, this fraction of incident radiation is not negligible. Thus, regarding laser safety, it is one of the main reasons why proper eye protection is always required (see Chap. 5).

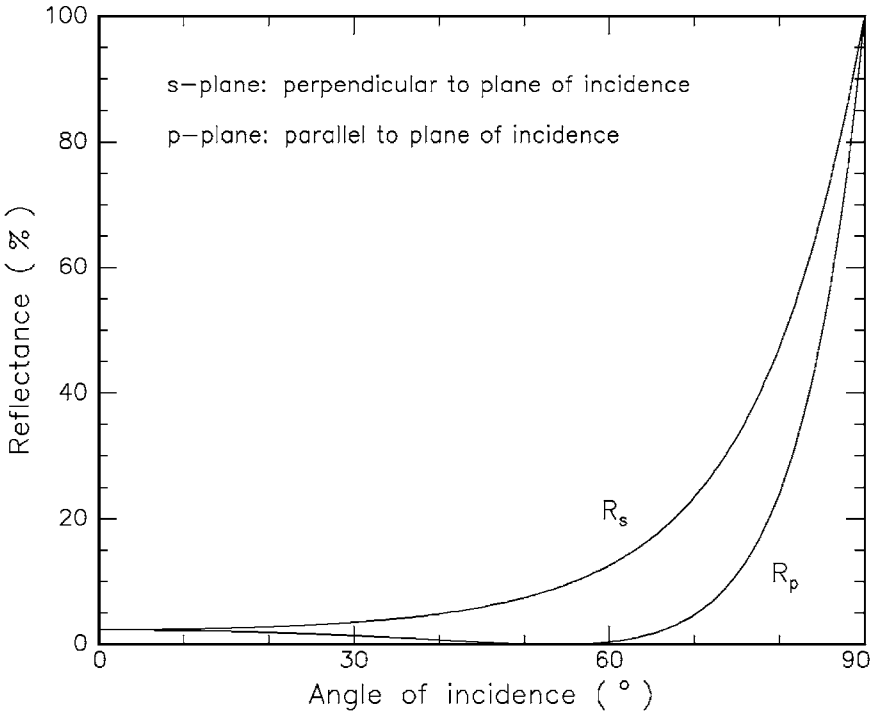

Fig. 2.3. Reflectances in s- and p-plane for water ($n = 1.33$)

For water, the indices of refraction and the corresponding reflectances at different wavelengths are listed in Table 2.1. Two strong absorption bands occur at about 2.9 μm and 6.0 μm. They result from vibrational and rotational oscillations of the water molecule. The major aspects of absorption will be addressed in the next section.

Table 2.1. Indices of refraction and reflectances of water. Data according to Hale and Querry (1973)

Wavelength λ (μm)	Index of refraction n	Reflectance R
0.2	1.396	0.027
0.3	1.349	0.022
0.4	1.339	0.021
0.5	1.335	0.021
0.6	1.332	0.020
0.7	1.331	0.020
0.8	1.329	0.020
0.9	1.328	0.020
1.0	1.327	0.020
1.6	1.317	0.019
2.0	1.306	0.018
2.6	1.242	0.012
2.7	1.188	0.007
2.8	1.142	0.004
2.9	1.201	0.008
3.0	1.371	0.024
3.1	1.467	0.036
3.2	1.478	0.037
3.3	1.450	0.034
3.4	1.420	0.030
3.5	1.400	0.028
4.0	1.351	0.022
5.0	1.325	0.020
6.0	1.265	0.014
7.0	1.317	0.019
8.0	1.291	0.016
9.0	1.262	0.013
10.0	1.218	0.010

Even if the dependence of the index of refraction on wavelength is rather weak in the visible spectrum, it should be taken into account when striving for predictable results. In general, indices of refraction for various kinds of tissue are difficult to measure due to absorption and scattering. Reflection from these tissues must be obtained empirically. In most cases, the corresponding indices of the refraction of water are rough estimates only.

2.2 Absorption

During *absorption*, the intensity of an incident electromagnetic wave is attenuated in passing through a medium. The *absorbance* of a medium is defined as the ratio of absorbed and incident intensities. Absorption is due to a partial conversion of light energy into heat motion or certain vibrations of molecules of the absorbing material. A perfectly *transparent* medium permits the passage of light without any absorption, i.e. the total radiant energy entering into and emerging from such a medium is the same. Among biological tissues, cornea and lens can be considered as being highly transparent for visible light. In contrast, media in which incident radiation is reduced practically to zero are called *opaque*.

The terms "transparent" and "opaque" are relative, since they certainly are wavelength-dependent. Cornea and lens, for instance, mainly consist of water which shows a strong absorption at wavelengths in the infrared spectrum. Hence, these tissues appear opaque in this spectral region. Actually, no medium is known to be either transparent or opaque to all wavelengths of the electromagnetic spectrum.

A substance is said to show *general absorption* if it reduces the intensity of all wavelengths in the considered spectrum by a similar fraction. In the case of visible light, such substances will thus appear grey to our eye. *Selective absorption*, on the other hand, is the absorption of certain wavelengths in preference to others. The existence of colors actually originates from selective absorption. Usually, *body colors* and *surface colors* are distinguished. Body color is generated by light which penetrates a certain distance into the substance. By backscattering, it is then deviated and escapes backwards from the surface but only after being partially absorbed at selected wavelengths. In contrast, surface color originates from reflection at the surface itself. It mainly depends on the reflectances which are related to the wavelength of incident radiation by (2.12).

The ability of a medium to absorb electromagnetic radiation depends on a number of factors, mainly the electronic constitution of its atoms and molecules, the wavelength of radiation, the thickness of the absorbing layer, and internal parameters such as the temperature or concentration of absorbing agents. Two laws are frequently applied which describe the effect of either thickness or concentration on absorption, respectively. They are commonly called *Lambert's law* and *Beer's law*, and are expressed by

$$I(z) = I_0 \exp(-\alpha z) \ , \tag{2.13}$$

and

$$I(z) = I_0 \exp(-k'cz) \ , \tag{2.14}$$

where z denotes the optical axis, $I(z)$ is the intensity at a distance z, I_0 is the incident intensity, α is the absorption coefficient of the medium, c is the

concentration of absorbing agents, and k' depends on internal parameters other than concentration. Since both laws describe the same behavior of absorption, they are also known as the *Lambert–Beer law*. From (2.13), we obtain

$$z = \frac{1}{\alpha} \ln \frac{I_0}{I(z)} \ . \tag{2.15}$$

The inverse of the absorption coefficient α is also referred to as the absorption length L, i.e.

$$L = \frac{1}{\alpha} \ . \tag{2.16}$$

The absorption length measures the distance z in which the intensity $I(z)$ has dropped to 1/e of its incident value I_0.

In biological tissues, absorption is mainly caused by either water molecules or macromolecules such as proteins and pigments. Whereas absorption in the IR region of the spectrum can be primarily attributed to water molecules, proteins as well as pigments mainly absorb in the UV and visible range of the spectrum. Proteins, in particular, have an absorption peak at approximately 280 nm according to Boulnois (1986). The discussion of the absorption spectrum of water – the main constituent of most tissues – will be deferred to Sect. 3.2 when addressing thermal interactions.

In Fig. 2.4, absorption spectra of two elementary biological absorbers are shown. They belong to melanin and hemoglobin (HbO_2), respectively. Melanin is the basic pigment of skin and is by far the most important epidermal chromophore. Its absorption coefficient monotonically increases across the visible spectrum toward the UV. Hemoglobin is predominant in vascularized tissue. It has relative absorption peaks around 280 nm, 420 nm, 540 nm, and 580 nm, and then exhibits a cut-off at approximately 600 nm. A general feature of most biomolecules is their complex band structure between 400 nm and 600 nm. Since neither macromolecules nor water strongly absorb in the near IR, a "therapeutic window" is delineated between roughly 600 nm and 1200 nm. In this spectral range, radiation penetrates biological tissues at a lower loss, thus enabling treatment of deeper tissue structures.

The absorption spectra of three typical tissues are presented in Fig. 2.5. They are obtained from the skin, aortic wall, and cornea, respectively. Among these, skin is the highest absorber, whereas the cornea is almost perfectly transparent[1] in the visible region of the spectrum. Because of the uniqueness of the absorption spectra, each of them can be regarded as a fingerprint of the corresponding tissue. Of course, slight deviations from these spectra can occur due to the inhomogeneity of most tissues.

[1] Actually, it is amazing how nature was able to create tissue with such transparency. The latter is due to the extremely regular structure of collagen fibrils inside the cornea and its high water content.

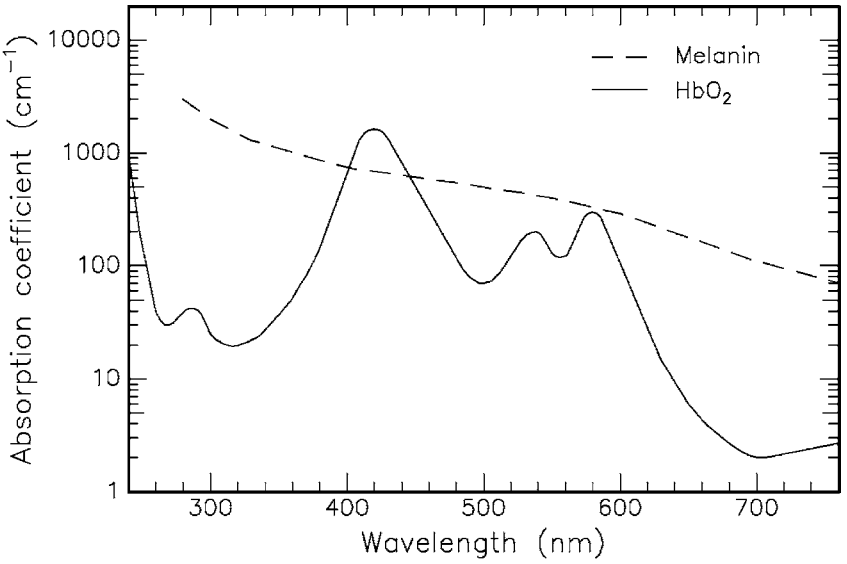

Fig. 2.4. Absorption spectra of melanin in skin and hemoglobin (HbO_2) in blood. Relative absorption peaks of hemoglobin are at 280 nm, 420 nm, 540 nm, and 580 nm. Data according to Boulnois (1986)

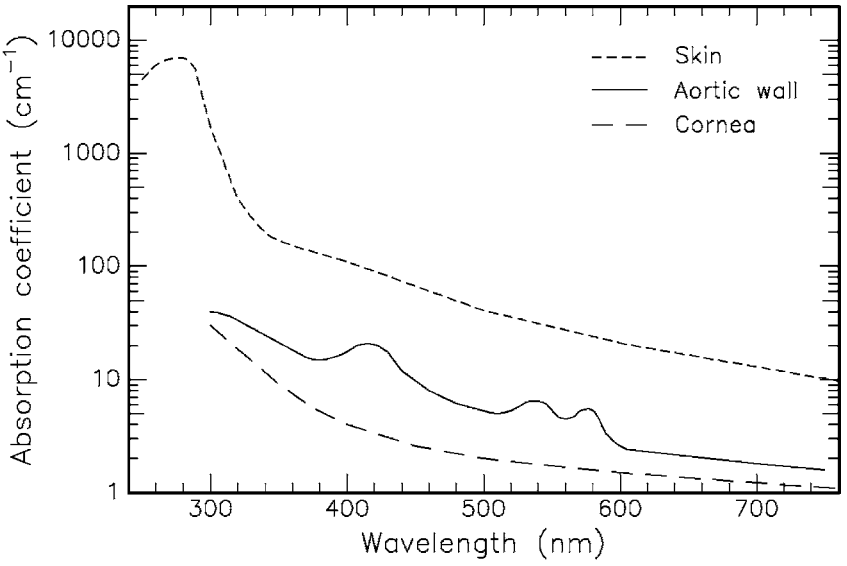

Fig. 2.5. Absorption spectra of skin, aortic wall, and cornea. In the visible range, the absorption of skin is 20–30 times higher than the absorption of corneal tissue. The absorption spectrum of aortic wall exhibits similar peaks as hemoglobin. Data according to Parrish and Anderson (1983), Keijzer et al. (1989), and Eichler and Seiler (1991)

When comparing Figs. 2.4 and 2.5, we find that the absorption spectra of the aortic wall and hemoglobin are quite similar. This observation can be explained by the fact that hemoglobin – as already previously stated – is predominant in vascularized tissue. Thus, it becomes evident that the same absorption peaks must be present in both spectra. Since the green and yellow wavelengths of krypton ion lasers at 531 nm and 568 nm, respectively, almost perfectly match the absorption peaks of hemoglobin, these lasers can be used for the coagulation of blood and blood vessels. For certain clinical applications, dye lasers may be an alternative choice, since their tunability can be advantageously used to match particular absorption bands of specific proteins and pigments.

Not only the absorption of biological tissue, though, is important for medical laser surgery. In certain laser applications, e.g. sclerostomies, special dyes and inks are frequently applied prior to laser exposure. By this means, the original absorption coefficient of the specific tissue is increased, leading to a higher efficiency of the laser treatment. Moreover, adjacent tissue is less damaged due to the enhanced absorption. For further details on sclerostomy, the reader is referred to Sect. 4.1.

In Table 2.2, the effects of some selected dyes on the damage threshold are demonstrated in the case of scleral tissue. The dyes were applied to the sclera by means of electrophoresis, i.e. an electric current was used to direct the dye into the tissue. Afterwards, the samples were exposed to picosecond pulses from a Nd:YLF laser to achieve optical breakdown (see Sect. 3.4). The absolute and relative threshold values of pulse energy are listed for each dye. Obviously, the threshold for the occurrence of optical breakdown can be decreased by a factor of two when choosing the correct dye. Other dyes evoked only a slight decrease in threshold or no effect at all. In general, the application of dyes should be handled very carefully, since some of them might induce toxic side effects.

Table 2.2. Effect of selected dyes and inks on damage threshold of scleral tissue. Damage was induced by a Nd:YLF laser (pulse duration: 30 ps, focal spot size: 30 μm). Unpublished data

Dye	Damage threshold (μJ)	Relative threshold
None	87	100 %
Erythrosine	87	100 %
Nigrosine	87	100 %
Reactive black	82	94 %
Brilliant black	81	93 %
Amido black	75	86 %
Methylene blue	62	71 %
Tatrazine	62	71 %
Bismarck brown	56	64 %
India ink	48	55 %

2.3 Scattering

When elastically bound charged particles are exposed to electromagnetic waves, the particles are set into motion by the electric field. If the frequency of the wave equals the natural frequency of free vibrations of a particle, resonance occurs being accompanied by a considerable amount of absorption. *Scattering*, on the other hand, takes place at frequencies not corresponding to those natural frequencies of particles. The resulting oscillation is determined by forced vibration. In general, this vibration will have the same frequency and direction as that of the electric force in the incident wave. Its amplitude, however, is much smaller than in the case of resonance. Also, the phase of the forced vibration differs from the incident wave, causing photons to slow down when penetrating into a denser medium. Hence, scattering can be regarded as the basic origin of dispersion.

Elastic and *inelastic scattering* are distinguished, depending on whether part of the incident photon energy is converted during the process of scattering. In the following paragraphs, we will first consider elastic scattering, where incident and scattered photons have the same energy. A special kind of elastic scattering is *Rayleigh scattering*. Its only restriction is that the scattering particles be smaller than the wavelength of incident radiation. In particular, we will find a relationship between scattered intensity and index of refraction, and that scattering is inversely proportional to the fourth power of wavelength. The latter statement is also known as *Rayleigh's law* and shall be derived in the following paragraphs.

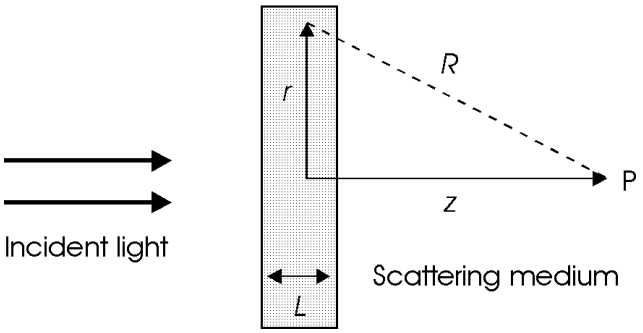

Fig. 2.6. Geometry of Rayleigh scattering

In Fig. 2.6, a simple geometry of Rayleigh scattering is shown. A plane electromagnetic wave is incident on a thin scattering medium with a total thickness L. At a particular time, the electric field of the incident wave can be expressed by

$$E(z) = E_0 \ \exp(\mathrm{i}kz) \ ,$$

where E_0 is the amplitude of the incident electric field, k is the amount of the propagation vector, and z denotes the optical axis. In a first approximation, we assume that the wave reaching some point P on the optical axis will essentially be the original wave, plus a small contribution due to scattering. The loss in intensity due to scattering is described by a similar relation as absorption, i.e.

$$I(z) = I_0 \ \exp(-\alpha_\mathrm{s} z) \ , \tag{2.17}$$

where α_s is the scattering coefficient. Differentiation of (2.17) with respect to z leads to

$$\mathrm{d}I = -\alpha_\mathrm{s} I \, \mathrm{d}z \ .$$

The intensity scattered by a thin medium of a thickness L as shown in Fig. 2.6 is thus proportional to α_s and L:

$$I_\mathrm{s} \sim \alpha_\mathrm{s} L \ . \tag{2.18}$$

Let us now assume that there are NL atoms per unit area of the scattering medium. Herein, the parameter N shall denote the density of scattering atoms. Then, the intensity scattered by one of these atoms can be described by the relation

$$I_1 \sim \frac{\alpha_\mathrm{s} L}{NL} = \frac{\alpha_\mathrm{s}}{N} \ .$$

Thus, the amplitude of the corresponding electric field is

$$E_1 \sim \sqrt{\frac{\alpha_\mathrm{s}}{N}} \ .$$

Due to the interference of all scattered waves, the total scattered amplitude can be expressed by

$$E_\mathrm{s} \sim NL \sqrt{\frac{\alpha_\mathrm{s}}{N}} = L\sqrt{\alpha_\mathrm{s} N} \ .$$

The complex amplitude at a distance z on the optical axis is obtained by adding the amplitudes of all scattered spherical waves to the amplitude of the incident plane wave, i.e.

$$E(z) = E_0 \left(\mathrm{e}^{\mathrm{i}kz} + L\sqrt{\alpha_\mathrm{s} N} \int_0^\infty \frac{\mathrm{e}^{\mathrm{i}kR}}{R} \ 2\pi r \ \mathrm{d}r \right) \ , \tag{2.19}$$

with $\quad R^2 = z^2 + r^2 \ .$

At a given z, we thus obtain

$$r \ \mathrm{d}r = R \ \mathrm{d}R \ ,$$

which reduces (2.19) to

$$E(z) = E_0 \left(\mathrm{e}^{\mathrm{i}kz} + L\sqrt{\alpha_\mathrm{s} N}\, 2\pi \int_z^\infty \mathrm{e}^{\mathrm{i}kR}\, \mathrm{d}R \right) . \tag{2.20}$$

Since wave trains always have a finite length, scattering from $R \to \infty$ can be neglected. Hence, (2.20) turns into

$$E(z) = E_0 \left(\mathrm{e}^{\mathrm{i}kz} - L\sqrt{\alpha_\mathrm{s} N}\, \frac{2\pi}{\mathrm{i}k}\, \mathrm{e}^{\mathrm{i}kz} \right) ,$$

and when inserting the wavelength $\lambda = 2\pi/k$

$$E(z) = E_0\, \mathrm{e}^{\mathrm{i}kz} \left(1 + \mathrm{i}\lambda L\sqrt{\alpha_\mathrm{s} N} \right) . \tag{2.21}$$

According to our assumption, the contribution of scattering – i.e. the second term in parentheses in (2.21) – is small compared to the first. Hence, they can be regarded as the first two terms of an expansion of

$$E(z) = E_0 \exp\left[\mathrm{i} \left(kz + \lambda L\sqrt{\alpha_\mathrm{s} N} \right) \right] .$$

Therefore, the phase of the incident wave is altered by the amount $\lambda L\sqrt{\alpha_\mathrm{s} N}$ due to scattering. This value must be equal to the well-known expression of phase retardation given by

$$\Delta\phi = \frac{2\pi}{\lambda}\, (n-1)L ,$$

which occurs when light enters from free space into a medium with refractive index n. Hence,

$$\lambda L\sqrt{\alpha_\mathrm{s} N} = \frac{2\pi}{\lambda}(n-1)L ,$$

$$n - 1 = \frac{\lambda^2}{2\pi}\sqrt{\alpha_\mathrm{s} N} . \tag{2.22}$$

From (2.18) and (2.22), we finally obtain *Rayleigh's law* of scattering when neglecting the wavelength-dependence of n, i.e.

$$I_\mathrm{s} \sim \frac{1}{\lambda^4} . \tag{2.23}$$

If the scattering angle θ is taken into account, a more detailed analysis yields

$$I_\mathrm{s}(\theta) \sim \frac{1 + \cos^2(\theta)}{\lambda^4} , \tag{2.24}$$

where $\theta = 0$ denotes forward scattering. Rayleigh's law is illustrated in Fig. 2.7. Within the visible spectrum, scattering is already significantly reduced when comparing blue and red light.

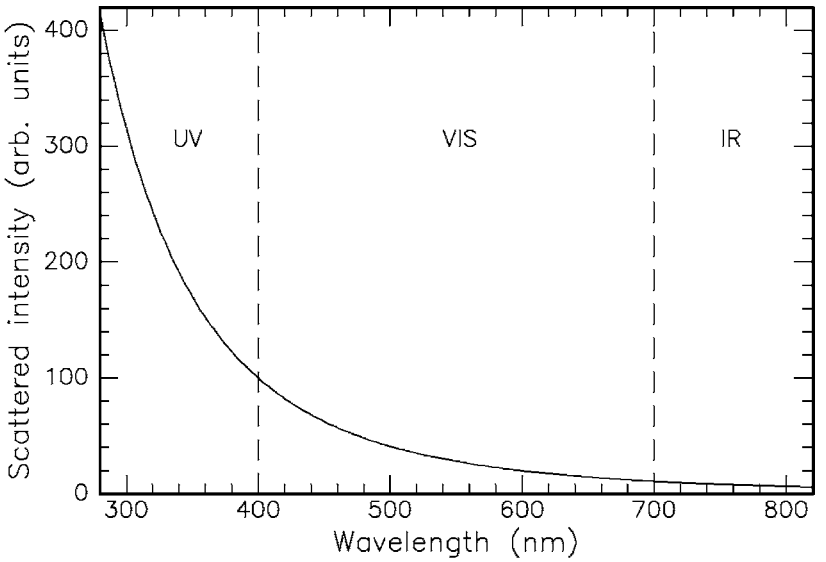

Fig. 2.7. Rayleigh's law of scattering for near UV, visible, and near IR light

Rayleigh scattering is elastic scattering, i.e. scattered light has the same values of k and λ as incident light. One important type of inelastic scattering is known as *Brillouin scattering*. It arises from acoustic waves propagating through a medium, thereby inducing inhomogeneities of the refractive index. Brillouin scattering of light to higher (or lower) frequencies occurs, because scattering particles are moving toward (or away from) the light source. It can thus be regarded as an optical *Doppler effect* in which the frequency of photons is shifted up or down. In laser–tissue interactions, Brillouin scattering becomes significant only during the generation of shock waves as will be discussed in Sect. 3.5.

In our derivation of Rayleigh's law, absorption has been neglected. Therefore, (2.22) – (2.24) are valid only for wavelengths far away from any absorption bands. Simultaneous absorption and scattering will be discussed in Sect. 2.4. Moreover, we did not take the spatial extent of scattering particles into account. If this extent becomes comparable to the wavelength of the incident radiation such as in blood cells, Rayleigh scattering no longer applies and another type of scattering called *Mie scattering* occurs. The theory of Mie scattering is rather complex and shall thus not be repeated here. However, it is emphasized that Mie scattering and Rayleigh scattering differ in two important respects. First, Mie scattering shows a weaker dependence on wavelength ($\sim \lambda^{-x}$ with $0.4 \leq x \leq 0.5$) compared to Rayleigh scattering ($\sim \lambda^{-4}$). Second, Mie scattering preferably takes place in the forward direction, whereas Rayleigh scattering is proportional to $1 + \cos^2(\theta)$ according to (2.24), i.e. forward and backward scattered intensities are the same.

In most biological tissues, it was found by Wilson and Adam (1983), Jacques et al. (1987b), and Parsa et al. (1989) that photons are preferably scattered in the forward direction. This phenomenon cannot be explained by Rayleigh scattering. On the other hand, the observed wavelength-dependence is somewhat stronger than predicted by Mie scattering. Thus, neither Rayleigh scattering nor Mie scattering completely describe scattering in tissues. Therefore, it is very convenient to define a *probability function* $p(\theta)$ of a photon to be scattered by an angle θ which can be fitted to experimental data. If $p(\theta)$ does not depend on θ, we speak of *isotropic scattering*. Otherwise, *anisotropic scattering* occurs.

A measure of the anisotropy of scattering is given by the coefficient of anisotropy g, where $g = 1$ denotes purely forward scattering, $g = -1$ purely backward scattering, and $g = 0$ isotropic scattering. In polar coordinates, the coefficient g is defined by

$$g = \frac{\int_{4\pi} p(\theta)\ \cos\theta\ \mathrm{d}\omega}{\int_{4\pi} p(\theta)\ \mathrm{d}\omega}\ , \tag{2.25}$$

where $p(\theta)$ is a probability function and $\mathrm{d}\omega = \sin\theta\,\mathrm{d}\theta\,\mathrm{d}\phi$ is the elementary solid angle. By definition, the coefficient of anisotropy g represents the average value of the cosine of the scattering angle θ. As a good approximation, it can be assumed that g ranges from 0.7 to 0.99 for most biological tissues. Hence, the corresponding scattering angles are most frequently between 8° and 45°. The important term in (2.25) is the probability function $p(\theta)$. It is also called the *phase function* and is usually normalized by

$$\frac{1}{4\pi}\int_{4\pi} p(\theta)\ \mathrm{d}\omega = 1\ . \tag{2.26}$$

Several theoretical phase functions $p(\theta)$ have been proposed and are known as *Henyey–Greenstein*, *Rayleigh–Gans*, *δ–Eddington*, and *Reynolds* functions[2]. Among these, the first is best in accordance with experimental observations. It was introduced by Henyey and Greenstein (1941) and is given by

$$p(\theta) = \frac{1 - g^2}{(1 + g^2 - 2g\ \cos\theta)^{3/2}}\ . \tag{2.27}$$

This phase function is mathematically very convenient to handle, since it is equivalent to the representation

$$p(\theta) = \sum_{i=0}^{\infty}(2i + 1)\, g^i\, P_i(\cos\theta)\ , \tag{2.28}$$

[2] Detailed information on these phase functions is provided in the reports by Henyey and Greenstein (1941), van de Hulst (1957), Joseph et al. (1976), and Reynolds and McCormick (1980).

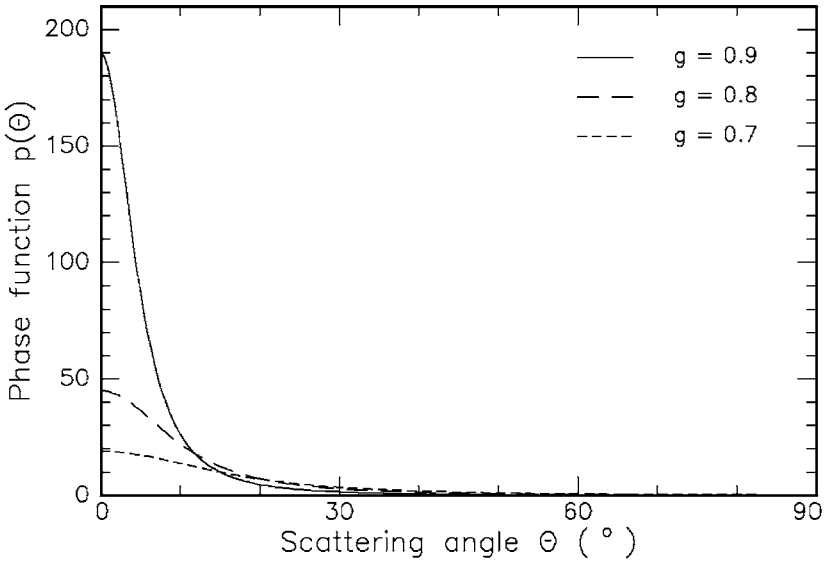

Fig. 2.8. Henyey–Greenstein function for different coefficients of anisotropy ranging from $g = 0.7$ to $g = 0.9$

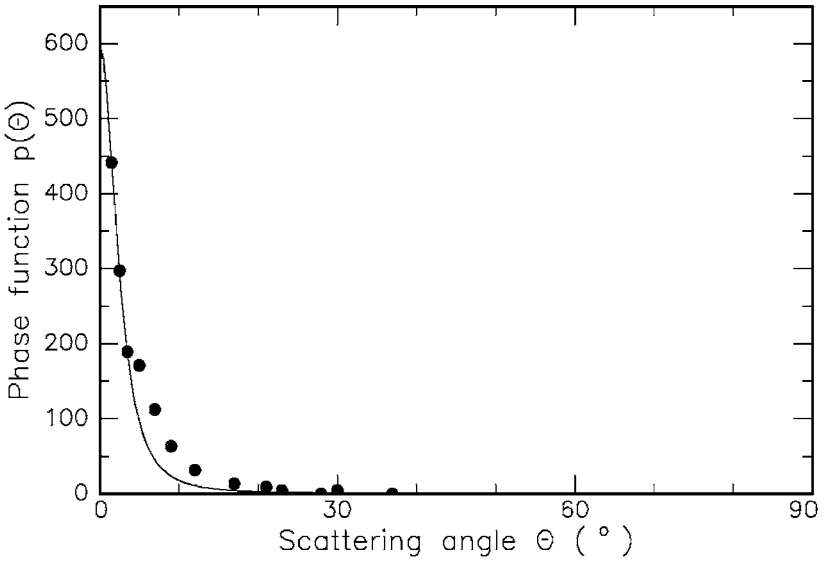

Fig. 2.9. Phase function for an 80 µm thick sample of aortic wall. The data are fitted to a composite function consisting of an isotropic term u and the anisotropic Henyey–Greenstein function (fit parameters: $g = 0.945$, $u = 0.071$). Data according to Yoon et al. (1987)

where P_i are the Legendre polynomials. In some cases, though, a composite function of an isotropic term u and the Henyey–Greenstein function does fit better to experimental data. According to Yoon et al. (1987), this modified function can be expressed by

$$p(\theta) = \frac{1}{4\pi} \; \frac{u + (1-u)\,(1-g^2)}{(1+g^2-2g\,\cos\theta)^{3/2}} \; . \tag{2.29}$$

In Fig. 2.8, the Henyey–Greenstein phase function is graphically shown for different values of g. Obviously, it describes the dominant process of scattering in the forward direction very well. In Fig. 2.9, experimental data are plotted for an 80 µm sample of aortic tissue. The data are fitted to the modified Henyey–Greenstein function as determined by (2.29) with the parameters $g = 0.945$ and $u = 0.071$.

2.4 Turbid Media

In the previous two sections, we have considered the occurrences of either absorption or scattering. In most tissues, though, both of them will be present simultaneously. Such media are called *turbid media*. Their total attenuation coefficient can be expressed by

$$\alpha_\mathrm{t} = \alpha + \alpha_\mathrm{s} \; . \tag{2.30}$$

In turbid media, the mean free optical path of incident photons is thus determined by

$$L_\mathrm{t} = \frac{1}{\alpha_\mathrm{t}} = \frac{1}{\alpha + \alpha_\mathrm{s}} \; . \tag{2.31}$$

Only in some cases, either α or α_s may be negligible with respect to each other, but it is important to realize the existence of both processes and the fact that usually both are operating. Also, it is very convenient to define an additional parameter, the *optical albedo* a, by

$$a = \frac{\alpha_\mathrm{s}}{\alpha_\mathrm{t}} = \frac{\alpha_\mathrm{s}}{\alpha + \alpha_\mathrm{s}} \; . \tag{2.32}$$

For $a = 0$, attenuation is exclusively due to absorption, whereas in the case of $a = 1$ only scattering occurs. For $a = 1/2$, (2.32) can be turned into the equality $\alpha = \alpha_\mathrm{s}$, i.e. the coefficients of absorption and scattering are of the same magnitude. In general, both effects will take place but they will occur in variable ratios.

In Fig. 2.10, the albedo is shown as a function of the scattering coefficient. Three different absorption coefficients are assumed which are typical for biological tissue. In addition, the value $a = 1/2$ is indicated. For $\alpha_\mathrm{s} >> \alpha$, the albedo asymptotically approaches unity.